

Wall coating optimization for microchannel reactors

A. Stefanescu^a, A.C. van Veen^a, C. Mirodatos^{a,*}, J.C. Beziat^b, E. Duval-Brunel^b

^aIRC-CNRS, 2 Av. Albert Einstein, 69626 Villeurbanne Cedex, France

^bRENAULT, Technocentre Direction de la Recherche, 1 av. du Golf 78288 Guyancourt, France

Available online 9 April 2007

Abstract

Thick and porous aluminum oxide coatings on the inner walls of a microchannel reactor have been developed as a support for catalytically active metals serving for on-board hydrogen production. These coatings must withstand extremely severe conditions in terms of temperature and mechanical shock. The developed suspension coating method uses alumina prepared from commercial powders. Optimizing the slurry preparation parameters such as particle size, viscosity, solid loading and/or binder content in tight relationship with coating properties allowed us to attain films at a desired thickness of 25 μm , with a good adhesion and reasonable uniformity. An ongoing investigation in our laboratory confirms that these coatings impregnated with an active phase can be successfully employed for hydrogen production by steam reforming of isooctane.

© 2007 Elsevier B.V. All rights reserved.

Keywords: Catalyst deposition; Alumina wash-coating; Microstructure; Steam reforming; Micro-structured reactors; Micro-reactors

1. Introduction

The development of catalytic microchannel reactors is today a matter of active research in catalytic reaction engineering and process intensification. A key feature of this kind of device is that mastering catalyst properties, i.e. morphology, activity, kinetics and stability, and the way to deposit and activate the catalytically active phases are inseparable from the choice of the microreactor geometry. As a matter of fact, in the global performance of the microreactor, catalyst and reactor are strongly intertwined. In consequence, the optimization must be done in an integral approach from the molecular to the reactor level. Until now, the mainstream of studies available in open literature presents only the microreactor's catalytic performance without explicit details about the catalyst development or characteristics. The rare publications where the coatings on microchannel metallic platelets were discussed evoked no more than the preparation methods [1–6].

The most common way to deposit catalysts within the microchannel channel is the wash-coating technique. For example, the commercially available $\text{CuO}/\text{ZnO}/\text{Al}_2\text{O}_3$ catalyst is one of the most studied system for hydrogen production by

methanol steam reforming (SRM) for feeding proton exchange membrane fuel cells (PEMFC) [7], or polymer electrolyte fuel cells [8]. Methods to control the thickness from 1 to 25 μm of a liquid film coating using controlled gelation of boehmite slurry have been developed. The effect of the Cu to Zn ratio, the impact of metal loading, and the effect of calcination temperature have been investigated to optimize the catalyst for the SRM reaction. Other authors [9,10] performed similar studies replacing zinc with cerium. Furthermore, Germani et al. [11] performed a systematic study on the nature of binders used for coating a $\text{Cu}/\text{Zn}/\text{Al}$ catalyst into microchannels, and their influence on catalytic activity for the water gas shift (WGS) reaction. They concluded that binders play a major role on (i) slurry viscosity by their chemical structure but also through their molecular weight, (ii) coating adhesion and (iii) catalytic activity by redispersion of the active phase because of metal complexes formation.

Rebrov et al. [12] published a review article giving a detailed description of the procedure for preparing ZSM-5 catalysts for selective catalytic reduction of NO with ammonia. The coating thickness was adjusted varying the reaction temperature, the synthesis time, the $\text{H}_2\text{O}/\text{Si}$ and $\text{Si}/\text{template}$ ratios, as well as the orientation of the platelet with respect to the gravity vector. Afterwards, a ZSM-5 zeolite coating has been prepared with a zeolitic layer thickness of a single crystal, particularly suitable for the considered catalytic reaction.

* Corresponding author. Tel.: +33 472445366; fax: +33 472445399.

E-mail address: claudio.mirodatos@catalyse.cnrs.fr (C. Mirodatos).

A fundamental study concerning the preparation of porous alumina wash-coats in the microchannels focused on the pre-treatment of the microstructures, properties, and adhesion of the wash-coats was performed by Zapf et al. [13]. Anodic oxidation and thermal treatment of the microstructures significantly reduced the undesirable chlorine content, which was assumed to have deleterious effects on the catalyst activity. Good adhesion of the porous catalysts, deposited by a two-step wash-coating and wet impregnation process, was demonstrated by a mechanical test. The impregnated Cr_2O_3 within alumina wash-coat was homogeneously distributed in vertical (depth of the coating) and horizontal (at the coating's surface) directions, whereas the content of CuO decreased with the wash-coat depth and islands of accumulated material were observed on the coating surface. The activity of the $\text{CuO}/\text{Cr}_2\text{O}_3/\text{Al}_2\text{O}_3$ system was investigated for methanol steam reforming.

The present study is exclusively dedicated to catalyst/carrier coatings in a microreactor designed for on-board steam-reforming production of hydrogen for PEMFC powered vehicles. These catalysts must withstand extremely severe conditions: the system must be fully operational within a minute, i.e. reaching its operating temperature (800°C) after a cold-start, and must respond rapidly to varying loads. Significant load transients occur frequently as a result of acceleration, hills, highway cruising, etc. not to mention the mechanical shocks that the catalyst undergoes during its utilization.

The purpose of the present work is to optimize all the relevant coating parameters for getting a thick, porous and stable (adherent) support layer for the active catalysts. To evaluate these properties, various descriptors or criteria like the resistance to mechanical and thermal shocks and the surface enhancement factor will be defined and used. The next steps of the active phase deposition, activation, and the catalytic performance of the optimized system will be presented in upcoming papers.

2. Experimental

2.1. Synthesis of the wash-coat

For the preparation of the alumina slurries, commercial materials were employed. The so-called “solids” are gamma-alumina ($\gamma\text{-Al}_2\text{O}_3$, 99.97%/Alfa Aesar Johnson Matthey; particle size $3\text{ }\mu\text{m}$; surface area $85\text{ m}^2\text{ g}^{-1}$), and boehmite (AlOOH -Disperal S/Condea Chemie GmbH; particle size

$25\text{ }\mu\text{m}$, nano-sized in dispersed phase; surface area $180\text{ m}^2\text{ g}^{-1}$). The liquids used are distilled water (DI) and the “binders” acetic acid ($\text{CH}_3\text{CO}_2\text{H}$, glacial, 99+%/Alfa Aesar GmbH & Co KG) and acrylic acid ($\text{C}_3\text{H}_4\text{O}_2$, 99%/Aldrich). Water and acids were mixed at first, followed by the powders, which were added under vigorous stirring. The suspension was kept under stirring for 24 h prior to deposition at room temperature. Several samples were prepared by varying the solid loading (more solid = Solid(+) sample; less solid = Solid(−) sample) or the binder content (less binder = Binder(−) sample; even less binder = Binder(− −) sample) when compared to reference sample (Table 1).

2.2. Coating of microchannel platelets

The proposed wash-coating method consists of: (i) a chemical and thermal treatment of the microchannel platelets and (ii) the coating deposition.

2.2.1. Support pre-treatment

The Aluchrom microchannel platelets having the following dimensions: $70\text{ mm} \times 50\text{ mm} \times 1.5\text{ mm}$ were used as the support for alumina coating. There are 40 microchannels on each platelet having: 70 mm length $\times 500\text{ }\mu\text{m}$ width $\times 550\text{ }\mu\text{m}$ depth.

In order to eliminate impurities as well as organic compounds, a three-step treatment was applied [14] using acetone (CH_3COCH_3 , 99+%, Aldrich), acetic acid ($\text{CH}_3\text{CO}_2\text{H}$, glacial, 99+%/Alfa Aesar GmbH & Co KG), ammonium hydroxide (NH_4OH , 1.0N Standardized Solution, Aldrich), phosphoric acid (H_3PO_4 , 85 wt.%, Aldrich), and hydrogen peroxide (H_2O_2 , 29–32%, Alfa Aesar GmbH & Co KG). First, the platelets were washed with acetone (Treatment I). Next they were immersed in a bath of 5:1:1 DI water: H_2O_2 : NH_4OH and rinsed in DI water (Treatment II) followed by immersion in a solution of 5:1:1:1 DI water: H_2O_2 : H_3PO_4 : $\text{CH}_3\text{CO}_2\text{H}$ in an ultrasonic bath and DI rinsing with this second stage being repeated twice (Treatment III). The XPS analysis confirms a three-fold reduction of the carbon compounds after the chemical treatment (Treatment III) compared to a regular washing with acetone (Treatment I) (Table 2).

Subsequently, the microchannel platelets were annealed at 1200°C for 1 h at a heating rate of $5^\circ\text{C}/\text{min}$. This thermal treatment triggered the segregation of an alumina layer on the metallic surface. The XRD patterns clearly showed the peaks associated to α -alumina. Prior to starting the coating procedure,

Table 1
Composition of tested slurries in wt. %

	Water (wt. %)	Acrylic acid (wt. %)	Acetic acid (wt. %)	Boehmite (wt. %)	γ -Alumina (wt. %)	Solid loading (wt. %)	Binder ^a content (wt. %)
Reference	78	5	2	11	5	16	5
Binder(−)	79	3	2	11	5	16	3
Binder(− −)	81	2	2	11	5	16	2
Solid(−)	82	5	2	8	3	11	5
Solid(+)	67	5	2	19	8	27	5

^a Binder used in these slurries is acrylic acid because no adherence is observed for samples without acrylic acid.

Table 2
Quantitative XPS analysis of an Aluchrom platelet

	Ni (at.%)	Cr ^a (at.%)	Fe (at.%)	C (at.%)	O (at.%)	N (at.%)	Sn (at.%)	P (at.%)
Treatment I (acetone)	–	2.5	3.5	62.4	29.8	1.8	–	–
Treatment II	3.3	10.2	8.2	36.6	39.5	1.6	0.6	–
Treatment III	2.4	9.6	5.8	29.5	47.1	0.52	2.7	2.4

^a Cr 3s superpose on the Al 2s.

all the supports were washed with ethanol, removing any superficial impurities caused by manipulation.

2.2.2. Coating deposition

The coating was performed according the following four-step procedure:

- (i) The slurry was applied to the microchannels of the platelets by using a syringe. Even though the use of a syringe is not a commercially viable process in the production of bulk quantity of coated platelets, it is a convenient way to undergo catalyst deposition procedure at lab scale with good layer quality [15,16].
- (ii) Any excess of suspension was wiped off. It could be mentioned that conventional techniques using gas assisted fluid displacement in cylindrical geometries (monolith like) [17] cannot be used here with the open channel platelet geometry.
- (iii) The platelets were dried at ambient temperature in air.
- (iv) The coated microchannel platelets were calcined at 800 °C using a heating rate of 1 °C/min. The final temperature was held for 4 h.

2.3. Adhesion test

Till now, no certified method exists to quantify the adhesion of coatings on microstructures. Most often adhesion is evaluated using an ultrasonic technique [18]. In order to ensure a reliable evaluation of the coating adhesion under realistic working conditions, the following test was implemented: (i) first, thermal shocks (20–800 °C) are applied in an oven in order to simulate the start-up and shut-down procedure of an on-board reformer; (ii) then the samples are tested by applying ultrasonic impulsions in a petrol ether bath and regularly measuring the resulting weight loss, in order to simulate the impact of mechanical stress that an on-board reactor may endure during utilization. Referring to literature data [19,20], a weight loss between 0 and 10% is considered to indicate a stable coating.

2.4. Characterization techniques

The specific surface area of the samples was calculated from the N₂ adsorption by using the BET equation. Prior to surface area determination, powders were outgassed at 350 °C for 4 h.

The pore size distribution of each sample was determined by desorption isotherm measurements using an ASAP 2010M apparatus from Micromeritics.

The crystalline structure of γ -alumina phase was examined by X-ray diffraction in a Bruker (Siemens) D5005 apparatus (Cu K α radiation, 0.154 nm).

XPS analyses were performed with an SSI (Surface Science Instruments) 301 spectrophotometer using a monochromatic Al K α radiation. The binding energy of C 1s = 284.6 eV was used as an internal reference.

The morphology of different samples was examined using scanning electron microscopy (SEM) on a Hitachi S800. The samples were covered with a thin film of Au–Pd before analysis in order to avoid charge accumulation and to improve image contrast.

The rheological properties of the samples were measured using a Visco Basic Plus, Fungilab, S.A., rotational viscometer equipped with spindle model TL5 in a speed range of 0.3–100 rpm. Samples were sheared in increasing order of spindle speed. Three readings of the apparent viscosity were taken per sample. Shear rate (s^{−1}) was calculated based on the manufacturer's instructions, as follows: shear rate = 1.32 \times rpm.

A Microtrac S3500 Series Particle Size Analyzer with tri-laser technology was used in order to determine the particle size distribution of the samples in the range of 0.7–1000 μ m. A spherical shape of the particles was assumed. The percentage of particles having a certain size was measured from the total solid volume.

3. Results and discussion

3.1. Slurry characterization

Since the characteristics of the slurry have a significant influence on the coating properties, several parameters as solid loading and binder content were varied in order to obtain thick alumina coatings with good adhesion, large surface enhancement factor (SEF, calculated as the ratio between the surface area – S_{BET} – of the coated platelet to the geometric area of the platelet), and acceptable coating coverage.

3.1.1. Viscosity

3.1.1.1. Influence of shear rate. In general, when a well-dispersed diluted ceramic suspension is prepared from a Newtonian fluid like water, the viscosity behavior of the suspension also remains Newtonian. Therefore, for these suspensions the viscosity is expected to remain constant regardless of the shear rate. This behavior is observed for the freshly prepared samples only at low shear rates (lower than 6 s^{−1}), where the Brownian motion dominates and the

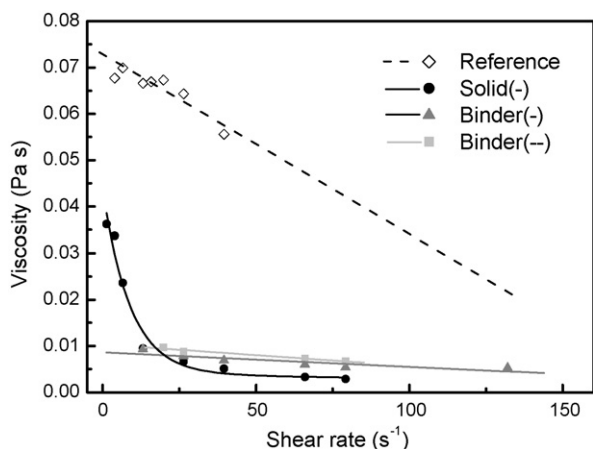


Fig. 1. Influence of shear rate on viscosity for freshly prepared samples.

structure of the suspensions remains relatively undisturbed, as shown in Fig. 1. Furthermore, as the shear rate increases, the particles structure in the suspensions is disturbed and the viscosity decreases leading to a “shear thinning”.

The sample having low solid loading, referred as Solid(–), presents a pronounced time-dependent pseudoplastic behavior, specific for paints and emulsions. This is most likely due to a higher acrylic acid versus solid ratio in the slurry; hence adding the binder polymers beyond the adsorption saturation limit can destabilize the slurry. In spite of many studies [21–23] regarding the electrostatic or electrosteric mechanism of alumina stabilization, the destabilizing effect of excess dispersant is not entirely understood. It is assumed that the destabilization may result from a “depletion flocculation” mechanism [21,24] or from a reduction of repulsive forces between particles [22].

The sample with a solid loading as high as 27 wt.%, Solid(+), “solidifies” instantaneously if stirring ceases.

3.1.1.2. Influence of time. The dependency of slurry viscosity with time at a constant shear rate of 19.8 s^{-1} is depicted in Fig. 2. It should be noted that the shearing was stopped between measurements, which prevents any direct conclusion about the

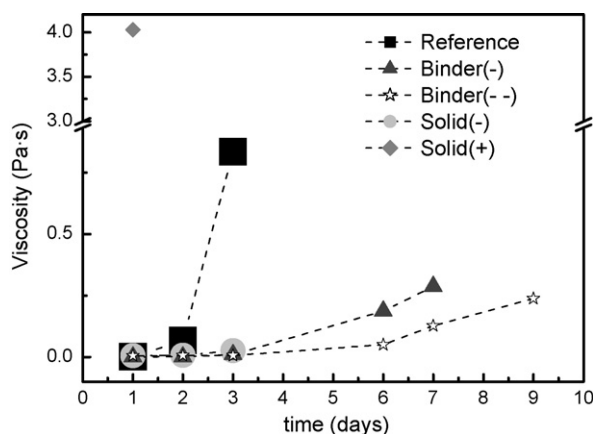


Fig. 2. Time dependence of viscosity at a constant shear rate of 19.8 s^{-1} .

rheologic behavior of the suspension (thixotropic or rheopectic). Viscosity increases gradually with time for all prepared samples, particularly for samples with high solid loading and acrylic acid concentration. This change is mainly due to the layered structure of boehmite, opening-up with time, resulting in an enlargement of the contact surface of solid with the liquid phase. Consequently, depletion in carboxylic group per solid surface occurs, followed by a decrease in electrostatic repulsion contributing to dispersion.

Subsequent to the initial viscosity measurements, all samples thereafter attained their original fluid state after vigorous stirring with a glass rod.

3.1.1.3. Influence of the acrylic acid concentration. The concentration of acrylic copolymers acting as binders/dispersants is a key factor in designing the dense alumina suspensions for ceramics fabrication [22,25]. However, no such dependency was observed for any of the prepared samples as shown in Fig. 3. This considerable difference can be attributed to the higher molar fraction of carboxylic groups present in the polymers used in literature studies: 55 versus 1 for acrylic acid.

3.1.2. Particle size

The particle size in the suspended powders is often described as the “principal factor”, affecting the characteristics of obtained wash-coat layers [26–28]. Therefore, much attention has been paid to the evolution of the particle size distribution with time, especially because solid materials with strongly differing particle size are employed for slurry preparations: gamma alumina, $3 \mu\text{m}$, and boehmite, $25 \mu\text{m}$, becoming nano-sized in the dispersed phase.

The particle size of the reference slurry measured at different time intervals (fresh slurry, 5 and 8 days aged slurry) is represented in Fig. 4(a). The particle size distribution of the slurry remains very stable and ranges from 0.3 to $11 \mu\text{m}$ throughout the whole period of observation due to a synergetic effect of alumina and boehmite particles. A possible explanation for this observable fact could be the adsorption of boehmite particles over alumina surface that modifies the surface characteristics [29]. Indeed, in the suspensions containing

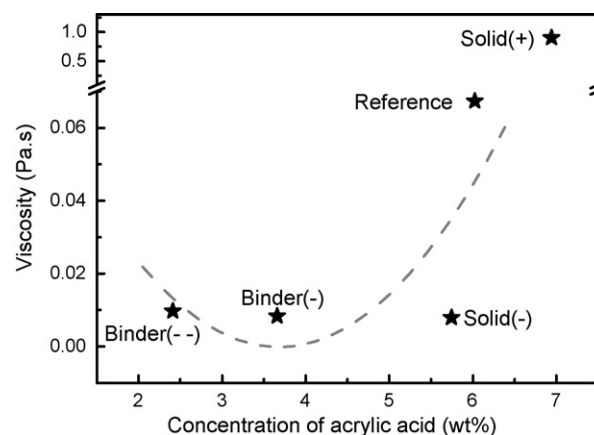


Fig. 3. Dependence of viscosity on the acrylic acid concentration (calculated in function of water wt.%) at a constant shear rate of 19.8 s^{-1} .

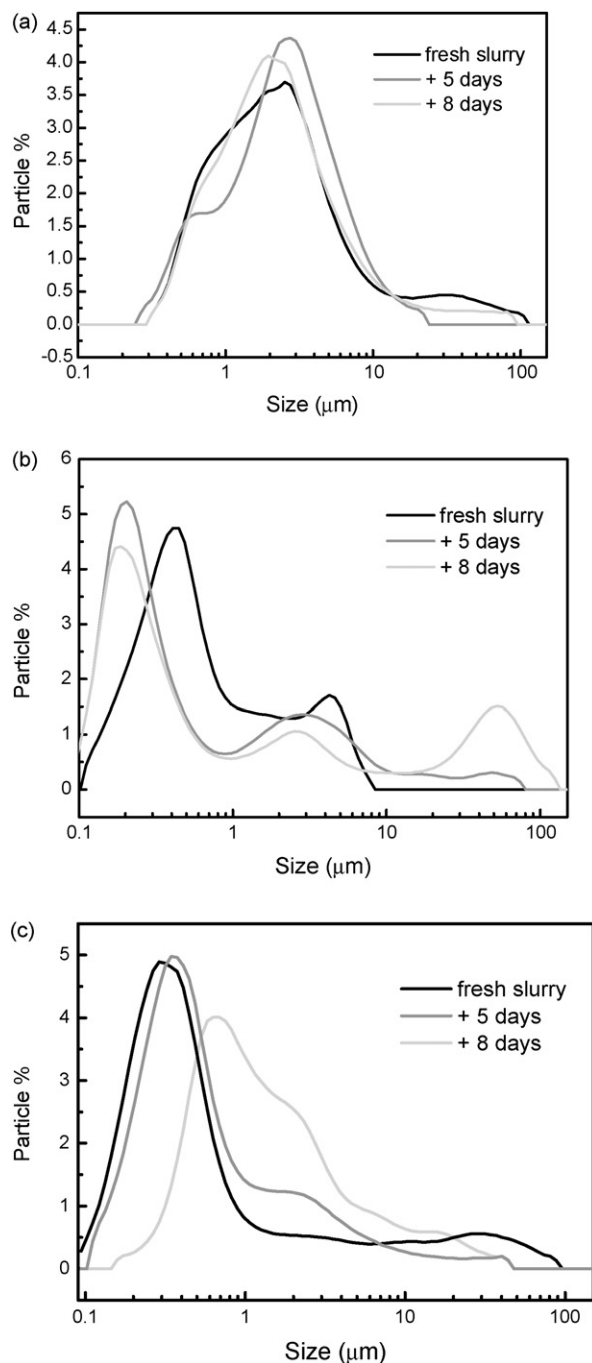


Fig. 4. Effect of slurry aging on the particle size distribution for the reference slurry (a), a slurry without alumina (b), and a slurry without boehmite (c).

only alumina (Fig. 4(c)) or only boehmite (Fig. 4(b)) a marked evolution of the particle size distribution with aging time is observed. In the case of the slurry containing only boehmite, for example, the initial monomodal distribution (centered around $0.8 \mu\text{m}$) tends after aging to become bi- or trimodal with small ($0.2 \mu\text{m}$), medium ($5 \mu\text{m}$) and very large ($80 \mu\text{m}$) particle size.

3.1.3. Effect of pH

The pH of the samples ranges from 3 to 3.5. Consequently, at this low pH range, the particle surface is positively charged

whereas the polyelectrolyte (acrylic acid) molecules are uncharged and have a low affinity for the solvent, which in turn results in a small (or) non-existent steric effect. Subsequently, deflocculating occurs from electrostatic repulsion between the particles [24].

Working at this low pH range presents several advantages:

- It keeps the boehmite in its dispersed form, the sol–gel transition taking place at pH values higher than 4 [30]. This in turn provides a reasonable fluidity of suspensions, even at high solid loading, since the boehmite behaves as a plasticizer [31] as well;
- the amount of polyelectrolyte adsorbed is increased due to the larger density of positive surface charges facilitating the anchoring of more carboxylic groups.

3.2. Impact of slurry parameters on coatings characteristics

A first set of coatings characterization has been presented in a previous paper by the same authors [32]. Briefly, the slurries are transformed into gamma alumina after calcination at 800°C for 4 h with a specific surface area as high as $149 \text{ m}^2 \text{ g}^{-1}$, and an average pore radius of 6.4 nm. The coatings present a satisfactory adhesion, a maximum of 7 wt.% of the total catalyst loading being lost during the test described in Section 2. The calculated SEF (surface enhancement factor), a key parameter for a coated microchannel platelet [33,34], is around $800 \text{ m}^2/\text{m}^2$ indicating that the wash-coat layer exposes an 800 times enlarged surface for the catalytic reaction.

In the following section, the coating thickness and the channel coverage will be discussed in function of several

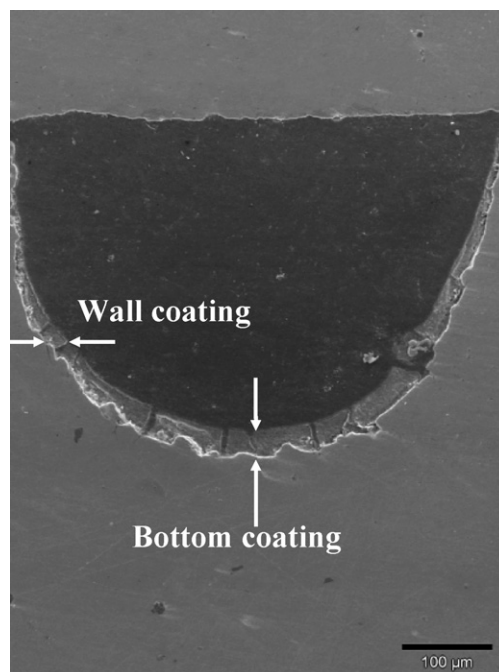


Fig. 5. SEM image of the alumina wash-coat in a channel cross-section view.

synthesis variables like viscosity, solid loading, binder content, and size of the channel.

3.2.1. Thickness

Up until recently, the only way to provide quantitative information on the thickness of coatings performed on microchannel platelets was the estimation based on the measured surface areas and layer density. This probably underestimated the thickness of the layer due to the decreased porosity of the coating [12]. The difficulty of measuring the “real” thickness occurs

mainly due to the unconformal (irregular) coverage of the coating inside the channel hollow—whether it is V or U shaped. This is typically true for coating methods using solvents.

We define the coating coverage as the ratio between wall coating thickness (W_{coating}) and bottom coating thickness (B_{coating}) (see Fig. 5). A channel having an optimum coating coverage presents a “coverage ratio” equal to unity.

Slurry synthesis parameters were varied in order to attain a coating with conformal coverage at a desired thickness of 25 μm . This targeted thickness was calculated by considering

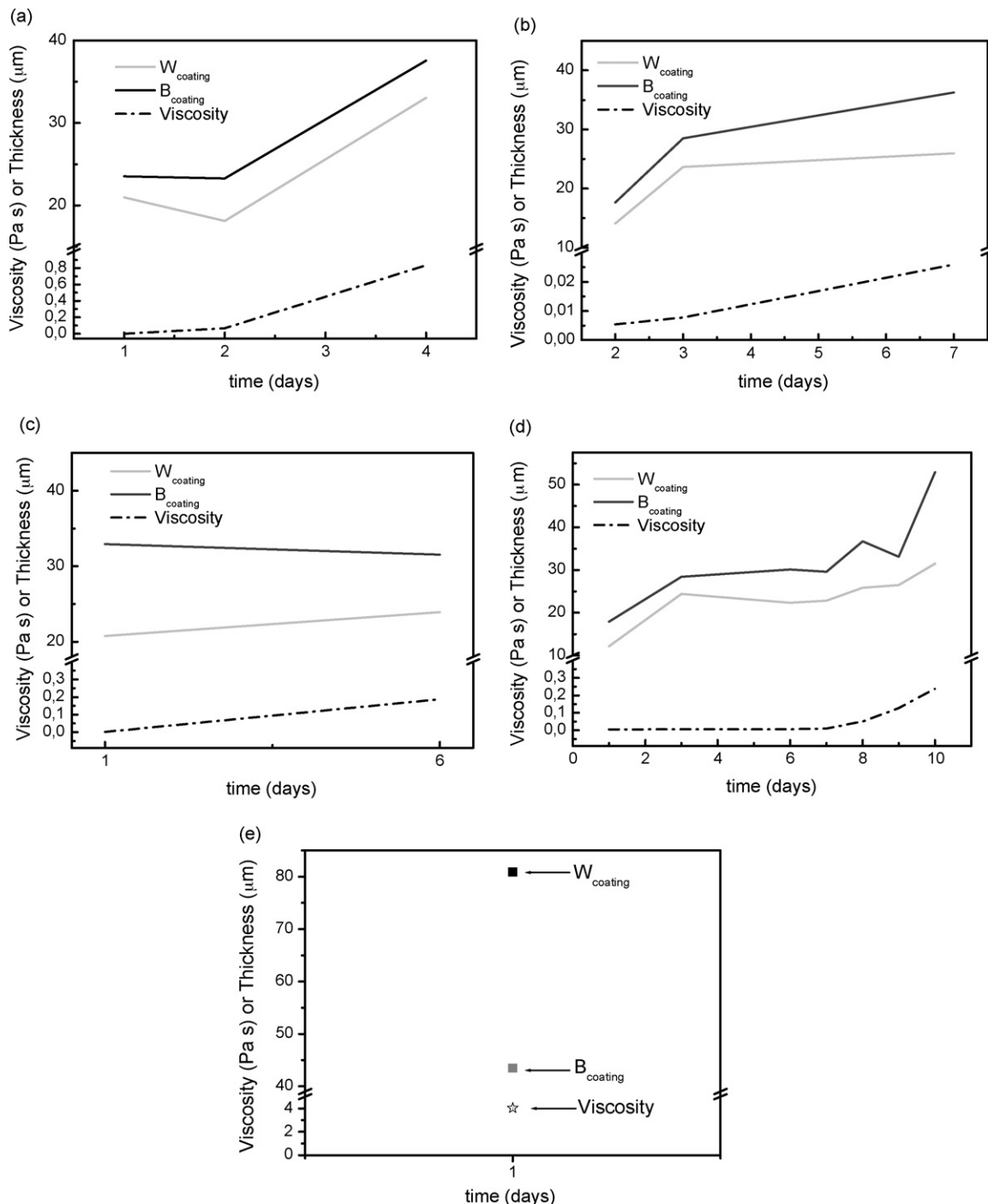


Fig. 6. Influence of slurry viscosity on the coating thickness for the reference sample (a), the Solid(–) sample (b), the Binder(–) sample (c), the Binder(– –) sample (d), and the Solid(+) sample (e).

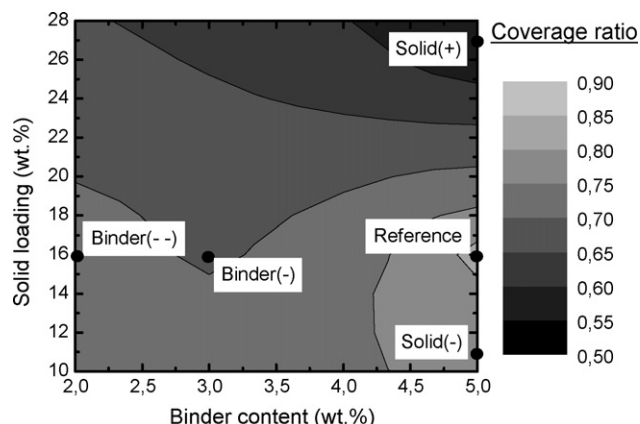


Fig. 7. “Coverage ratio” as a function of binder content and solid loading.

the amount of catalyst loading required at low radial temperature gradient for approaching the effluent composition determined by thermodynamics.

Relationships were established between the viscosity of slurries, coatings thickness and time was established, as shown in Fig. 6. The increase in viscosity yielded a higher thickness of coating, in spite of the solid loading or binder content. However, samples presenting lower viscosity offer the possibility to perform coating deposition for a longer period of time (up to 10 days for sample Binder(– –)), even though no major difference in thickness of the coating is noticed. On the contrary, when the solid loading is varied, a clear difference in terms of coating thickness is observed: reference sample 20–25 μm ; Solid(–) sample 15–20 μm and Solid(+) sample 40–80 μm , within the first day of slurries preparation (Fig. 6(a) and (b)). The solid loading influences the coating coverage in the channel (Fig. 7) as well. A reasonable equilibrium between binder content and solid loading is found only in the reference sample at a “coverage ratio” of 0.9.

Therefore, the reference sample represents a close-to-optimum coating for the final application in terms of thickness and coverage of the channel. Furthermore, a study regarding the coating coverage not only in channels along the platelets width, but also along the platelet length was performed using the Reference slurry (Fig. 8). It was demonstrated that the coating

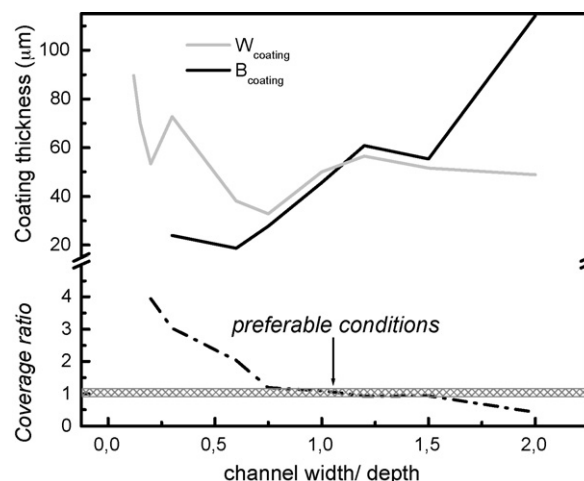


Fig. 9. “Coverage ratio” and coating thickness as a function of the channel geometry.

thickness at the bottom of the channel is lower at the edges of the platelet with a satisfactory “coverage ratio” at the center. This irregularity is due to the method of coating application, which is presently under investigation.

3.2.2. Coating in channels with variable geometry

The reference slurry was applied to a microchannel platelet with various channel widths: from 5 mm (channel 1) to 0.3 mm (channel 10), all having the same depth of 0.6 mm. An interesting relationship between the channel dimensions of the microchannel reactor/platelet and the uniformity of the coating was established (Fig. 9). The best coating coverage is found in the symmetrical channels where width and depth are both equal. In channels where the width is much larger than the depth, the coating presents a V shape, therefore allowing the deposition of a large amount of catalyst within this particular type of channel. This can be favorable in the case of slow catalytic reactions such as water gas shift conversion. If the channel depth is larger than the channel width, the coating presents a U shape, and the amount of deposited catalyst is smaller. This type of channel would be more appropriate for faster catalytic reactions such as steam reforming.

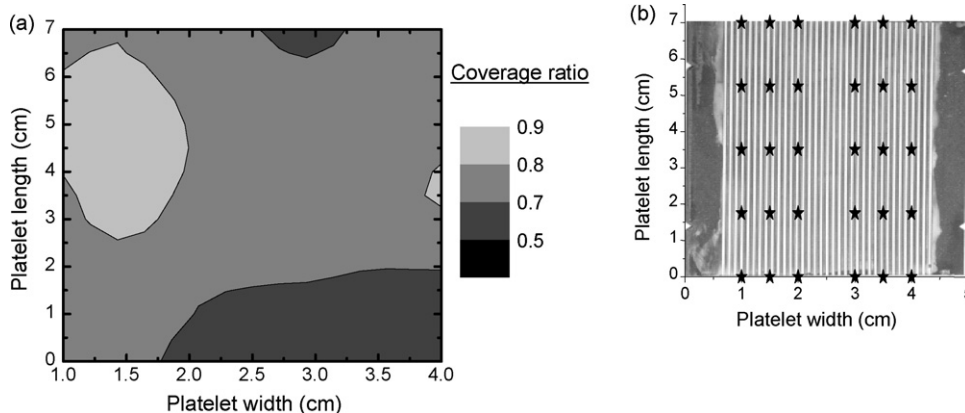


Fig. 8. (a) “Coverage ratio” over the platelet using the reference slurry; (b) positions of the 30 measurement spots for “coverage ratio”.

4. Conclusion

Viscosity, deposition time, particles size and pH have been varied by adjusting the binder and the solid content. The selected stable and homogeneous suspensions have been applied to microstructures after which the coatings were characterized in term of adhesion, composition, surface offered to the reaction, thickness, and uniformity. In this manner, a narrowed correlation between slurry preparation parameters versus coating properties was established. In addition, a study regarding the coating coverage of channels with different geometry demonstrated that the best uniformity is obtained in quasi-square channels.

Accordingly, a slurry recipe was selected for developing adherent and thick alumina layers having a good conformal coverage inside the channel and along the platelet. An ongoing study in our laboratory demonstrated that these coatings impregnated with nickel could be successfully used in steam reforming of hydrocarbons, such as isooctane, surrogating gasoline and diesel [32].

Acknowledgements

This work was supported by the “MISTRAL” Project (French Research Ministry). ATOTECH Deutschland GmbH is fully acknowledged for providing microchannel platelets and for helpful discussions.

References

- [1] M.T. Janicke, H. Kestenbaum, U. Hagendorf, F. Schuth, M. Fichtner, K. Schubert, *J. Catal.* 191 (2000) 282–293.
- [2] A. Rouge, B. Spoetzi, K. Gebauer, R. Schenk, A. Renken, *Chem. Eng. Sci.* 56 (2001) 1419–1427.
- [3] G. Germani, P. Alphonse, M. Courty, Y. Schuurman, C. Mirodatos, *Catal. Today* 110 (2005) 114–120.
- [4] A.R. Tadd, B.D. Gould, J.W. Schwank, *Catal. Today* 110 (2005) 68–75.
- [5] D. Truyen, M. Courty, P. Alphonse, F. Ansart, *Thin Solid Films* 495 (2006) 257–261.
- [6] Y.S.S. Wan, J.L.H. Chau, A. Gavrilidis, K.L. Yeung, *Micropor. Mesopor. Mater.* 42 (2001) 157–175.
- [7] J. Bravo, A. Karim, T. Conant, G.P. Lopez, A. Datye, *Chem. Eng. J.* 101 (2004) 113–121.
- [8] X. Yu, S.-T. Tu, Z. Wang, Y. Qi, *J. Power Sources* 150 (2005) 57–66.
- [9] Y. Men, H. Gnaser, C. Ziegler, R. Zapf, V. Hessel, G. Kolb, *Catal. Lett.* 105 (2005) 35–40.
- [10] Y. Men, H. Gnaser, R. Zapf, V. Hessel, C. Ziegler, *Catal. Commun.* 5 (2004) 671–675.
- [11] G. Germani, A. Stefanescu, Y. Schuurman, A.C. van Veen, *Chem. Eng. Sci.* (2007), doi:10.1016/j.ces.2007.02.034.
- [12] E.V. Rebrov, G.B.F. Seijger, H.P.A. Calis, M.H.J.M. de Croon, C.M. van den Bleek, J.C. Schouten, *Appl. Catal. A: Gen.* 206 (2001) 125–143.
- [13] R. Zapf, V. Hessel, G. Kolb, A. Ziogas, *Trans IChem: A* 81 (2003) 721–729.
- [14] R.S. Howell, M.K. Hoatalis, *J. Electrochem. Soc.* 149 (2002) G143–G146.
- [15] M.S. Lim, M.R. Kim, J. Noh, S.I. Woo, *J. Power Sources* 140 (2005) 66–71.
- [16] J.Y. Won, H.K. Jun, M.K. Jeon, S.I. Woo, *Catal. Today* 111 (2006) 158–163.
- [17] T. Conant, A. Karim, S. Rogers, S. Samms, G. Randolph, A. Datye, *Chem. Eng. Sci.* 61 (2006) 5678–5685.
- [18] Y.Y.S. Yasaki, K. Ihara, K. Ohkubo, US Patent 5,208,206, U.S.A. (1993).
- [19] A.V. Boix, J.M. Zamaro, E.A. Lombardo, E.E. Miro, *Appl. Catal. B: Environ.* 46 (2003) 121–132.
- [20] M. Valentini, G. Groppi, C. Cristiani, M. Levi, E. Tronconi, P. Forzatti, *Catal. Today* 69 (2001) 307–314.
- [21] J. Liu, W.Y. Shih, R. Kikuchi, I.A. Aksay, *J. Colloid Interf. Sci.* 142 (1991) 369–377.
- [22] Y. Fukuda, T. Togahi, Y. Suzuki, M. Naito, H. Kamiya, *Chem. Eng. Sci.* 56 (2001) 3005–3010.
- [23] A.S. Rao, *Ceram. Int.* 14 (1988) 17–25.
- [24] K. Vishista, F.D. Gnanam, *Mater. Lett.* 58 (2004) 1576–1581.
- [25] M.R.B. Romdhane, S. Boufi, S. Baklouti, T. Chartier, J.-F. Baumard, *Colloids Surf. A: Physicochem. Eng. Aspects* 212 (2003) 271–283.
- [26] C. Agrafiotis, A. Tsetsekou, A. Ekonomakou, *J. Mater. Sci. Lett.* 18 (1999) 1421–1424.
- [27] P. Pfeifer, K. Schubert, G. Emig, *Appl. Catal. A: Gen.* 286 (2005) 175–185.
- [28] C. Agrafiotis, A. Tsetsekou, *J. Eur. Ceram. Soc.* 20 (2000) 815–824.
- [29] I.H. Song, J.R.G. Evans, *J. Rheol.* 40 (1996) 131–152.
- [30] S. Ananthakumar, V. Raja, K.G.K. Warriar, *Mater. Lett.* 43 (2000) 174–179.
- [31] S. Ananthakumar, A.R.R. Menon, K. Prabhakaran, K.G.K. Warriar, *Ceram. Int.* 27 (2001) 231–237.
- [32] A. Stefanescu, A.C. van Veen, E. Duval-Brunel, C. Mirodatos, *Chem. Eng. Sci.* (2007), doi:10.1016/j.ces.2007.02.031.
- [33] I. Sandu, L. Presmanes, P. Alphonse, P. Tailhades, *Thin Solid Films* 495 (2006) 130–133.
- [34] K. Haas-Santo, M. Fichtner, K. Schubert, *Appl. Catal. A: Gen.* 220 (2001) 79–92.